Grain-boundary magnetoconductance and inelastic tunneling

M. Ziese and A. Bollero

Division of Superconductivity and Magnetism, University of Leipzig, 04103 Leipzig, Germany

I. Panagiotopoulos

Department of Materials Science and Engineering, University of Ioannina, Ioannina 45110, Greece

N. Moutis

Institute of Materials Science, NCSR "Demokritos," Ag. Paraskevi Attiki, 153 10, Greece

Measurements of the magnetoconductance of $La_{0.7}Sr_{0.3}MnO_3$ pressed powder samples in both the low and high field regime are reported. The magnetoconductance was calculated in a model based on inelastic tunneling via Mn sites situated in the tunneling barrier. This model satisfactorily accounts for the strong decrease of the low field magnetoconductance as a function of temperature due to spin depolarization in the inelastic tunneling processes. The susceptibility of the tunneling barrier was derived by two different methods showing the consistency of the model.

PACS number(s): 75.47.Gk, 75.70.−i, 73.50.Jt

I. INTRODUCTION

Grain-boundary magnetoconductance in manganites has been widely studied in recent years. This extrinsic magnetoconductance effect occurs in manganites and other magnetic oxides with extended defects. There are several features inherent in this transport mechanism that are virtually independent of the detailed defect structure. These include a steep conductance rise in moderate magnetic fields of the order of a few 10 mT, a strong decrease of this low field magnetoconductance with increasing temperature, a magnetoconductance depending linearly on magnetic field for fields in the Tesla range, and nonlinear current-voltage characteristics. Some models have been proposed to account for this behavior, see Ref. 1 for an overview. These agree on the significance of spin-polarized tunneling and inelastic tunneling processes in the understanding of the low field magnetoconductance as well as in the fact that the high field magnetoconductance is related to the magnetic properties of the tunneling barrier. However, the microscopic mechanisms of charge carrier transport in the grain-boundary region remain poorly understood. The existence of an insulating region near an extended defect has been attributed to bond angle variations disturbing the double exchange mechanism,[2] to the formation of a charge carrier depleted region due to some chemical potential variation,[3] or to phase separation at the internal interface.[4,5]

Since the manganites are highly spin-polarized materials, a large low field magnetoconductance up to 100% can be expected in a granular system.[6] Experimentally determined low field magnetoconductance values are, however, considerably lower and show a tendency to saturate at a level of 30%-40%.[7,8] This has been attributed to a depolarization of the carrier spins due to inelastic tunneling processes in the grain-boundary region.[7,8] Lee *et al.*[7] proposed a model for grain-boundary transport that includes tunneling via one impurity site in the barrier. This predicts a maximum magnetoconductance of 33% in low fields as well as a linear field dependence of the conductance in high fields in good agreement with the experimentally observed values. However, the magnetoconductance predicted by that model is proportional to the square of the saturation magnetization of the grains M_S^2 and has a temperature dependence much too weak in contrast to the strong decrease observed experimentally at temperatures far below the Curie temperature. One possibility to correct for this deficiency is to replace M_S^2 by an interfacial magnetization[9] M_I^2, since it has been experimentally shown[10] that M_I decreases much faster with temperature than M_S. However, this approach has two disadvantages, namely (1) the replacement is ad hoc and does not identify the underlying transport processes and (2) often the expressions derived in Ref. 7 are considered as universal, although these are an approximation in the limit of small grain-boundary magnetization that is only valid in not too strong fields. In this work this model will be extended to include higher order inelastic tunneling processes. This yields (1) an expression for the low field magnetoconductance with a temperature dependence in agreement with experiment and (2) identifies correction terms to the high field magnetoconductance. Recently systematic investigations of the grain-boundary magnetoconductance for a range of manganite compositions in high fields up to 50 T showed strong deviations from a linear field dependence in case of manganites with nonoptimal Curie temperature[11] in agreement with the results obtained here.

II. EXPERIMENT

$La_{0.7}Sr_{0.3}MnO_3$ (LSMO) powder samples were prepared by standard solid state reaction from stoichiometric amounts of high purity La_2O_3, $SrCO_3$, and Mn_2O_3 powders. The samples were calcined at 1000 °C for 12 h and subsequently sintered in air at 1400 °C for 5 d with two intermediate grindings and reformation into pellets. The final samples were obtained by high energy ball-milling for different durations from 1 to 27 h at 300 rpm and subsequent pressing into
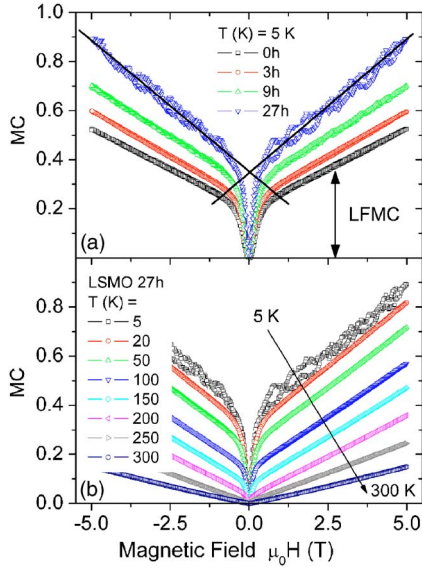
FIG. 1. (Color online) Magnetoconductance hysteresis curves measured (a) at 5 K on the samples milled for 0, 3, 9, and 27 h and (b) at various temperatures for the 27 h milled LSMO powder. The straight lines in (a) indicate the linear extrapolation of the high field conductance to determine the low field magnetoconductance LFMC.
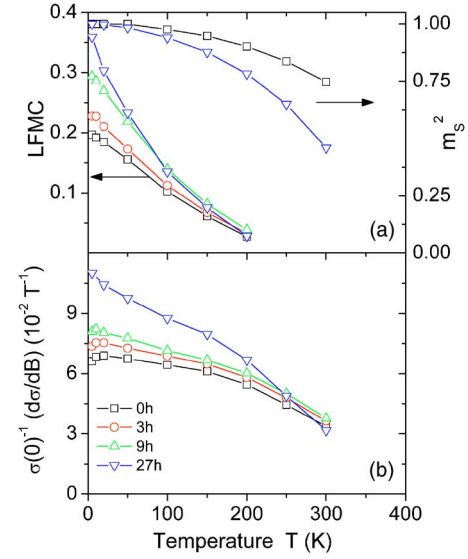

FIG. 2. (Color online) (a) Low field magnetoconductance LFMC of the samples with milling times 0, 3, 9, and 27 h. For comparison the normalized saturation magnetization m_S $=M_S(T)/M_S(0)$ of the samples with milling times 0 and 27 h is shown (right axis). (b) High field magnetoconductivity slope $d\sigma/dB$ of the same samples normalized to the zero field conductivity $\sigma(0)$.

pellets. The samples were characterized by x-ray diffractometry, scanning electron microscopy, scanning tunneling microscopy, superconducting quantum interference device (SQUID), and vibrating sample magnetometry as well as magnetotransport measurements.[12] A comparison of magnetoconductance

$$MC = \frac{\sigma(H) - \sigma(0)}{\sigma(0)} \qquad (1)$$

data measured at 5 K for the samples milled for 0, 3, 9, and 27 h is shown in Fig. 1(a). $\sigma(H)$ denotes the conductivity in an applied field H. The data show a steep low field magnetoconductance (LFMC) for magnetic fields below 0.5 T and a smooth high field magnetoconductance (HFMC) depending linearly on the magnetic field. With increasing milling time both the low field magnetoconductance as well as the high field conductance slope increase. Figure 1(b) shows the temperature dependence of the magnetoconductance of the sample milled for 27 h. Further experimental details can be found in Ref. 12.

From the data the high field magnetoconductivity slope $d\sigma/dB$ and the low field magnetoconductance value LFMC were determined. The standard extrapolation procedure used to determine the LFMC is indicated in Fig. 1(a).[13] Both LFMC and magnetoconductance slopes of the samples milled for 0, 3, 9, and 27 h are shown in Fig. 2. For comparison the reduced saturation magnetization m_S for the end members is shown in Fig. 2(a). The reduced magnetization m_S is defined as $m_S \equiv M_S(T)/M_S(0)$ with the saturation magnetization $M_S(T)$ of the grains which—to a good approximation—is identical to the measured magnetization. The saturation magnetization was extracted from magnetiza-

tion hysteresis curves using the following law of approach to saturation: $M = M_S[1 - (H_S/H)^2] + \chi H$. The LFMC decreases much stronger with increasing temperature than the square of the saturation magnetization.

III. THEORETICAL MODEL

A successful model for the grain-boundary magnetoconductance was proposed in Ref. 7. It is based on the double exchange transfer integral and includes inelastic tunneling processes via a single localized state in the barrier. In this case the conductivity σ is given by

$$\sigma \propto \langle (1 + \hat{s}_1 \cdot \hat{s}_b)(1 + \hat{s}_b \cdot \hat{s}_2) \rangle. \qquad (2)$$

$\hat{s}_i$, $i=1$, 2 and $\hat{s}_b$ denote unit vectors along the direction of the grain and grain-boundary spins, respectively. The charge carrier is assumed to move from core spin $\hat{s}_1$ in grain 1 to a grain-boundary spin $\hat{s}_b$ with an effective transfer integral proportional to $(1 + \hat{s}_1 \hat{s}_b)$ and then hop to core spin $\hat{s}_2$ in grain 2 with an equivalent transfer matrix element. The brackets indicate an ensemble average over the spin directions in the grains and the grain boundary. This is performed differently in the low and high field regime.

A. Low field regime

In zero field the orientation of both the grain-boundary spins and the grain magnetization is assumed to be random such that the zero field conductivity does not depend on the magnetization. Low fields will align the magnetization direction of the grains without changing the magnetic structure of the barrier significantly. A mean field approach is generally used to include the influence of thermal fluctuations and in

this case the unit vectors $\hat{s}_i$ are replaced by $m_S\hat{z}$, whereas $\hat{s}_b$ is still assumed to be a unit vector with random orientation. $\hat{z}$ is a unit vector along the field direction. Averaging yields

$$\sigma_1 \propto \left(1 + \tfrac{1}{3}m_S^2\right) \tag{3}$$

such that a magnetoconductance of $m_S^2/3$ is found in the low field limit. This model predicts a magnetoconductance of $1/3$ at low temperatures, since $m_S \to 1$ in this regime. This is in reasonable agreement with experimental data[7] and accounts for the fact that the observed low field magnetoconductance is always considerably lower than the value of 100% expected for a half-metallic granular system. However, the model fails in two aspects: (1) the low field magnetoconductance is predicted to scale with m_S^2, whereas the experimental results show a much stronger decrease with temperature, see Fig. 2(a); (2) higher order inelastic tunneling processes are not included, but clearly show up in the nonlinear current-voltage curves.[3,8,14,15] A model based on inelastic tunneling was proposed in Ref. 3 which explains the nonlinear current-voltage characteristics. However, since the barrier potential is assumed to be proportional to the difference in chemical potential $\Delta\mu \propto (M_{gb}^2 - M_S^2)$ the high field magnetoconductance is inevitably exponential in the square of the magnetic field, unless one makes the somewhat artificial assumption that $M_{gb} \propto \sqrt{H}$. The linearity of the high field magnetoconductance has been observed in LSMO up to 60 T.[9] Therefore the model of Ref. 7 appears to be more appropriate as a starting point for further refinement.

Here the model is extended to include higher order tunneling processes. A nth order tunneling process is defined as occurring via n sites in the grain boundary. In the low field case as above the grain boundary spins are assumed to have a random orientation, whereas the grain magnetization is given by $\hat{s}_i = m_S\hat{z}$. Then, in obvious notation, the nth order conductivity in the low field regime is given by

$$\sigma_n \propto \langle (1 + \hat{s}_1 \cdot \hat{s}_{b1})(1 + \hat{s}_{b1} \cdot \hat{s}_{b2}) \ldots (1 + \hat{s}_{bn} \cdot \hat{s}_2) \rangle \tag{4}$$

$$= 1 + \langle \hat{s}_1 \cdot \hat{s}_{b1} + \hat{s}_{b1} \cdot \hat{s}_{b2} \ldots \hat{s}_{bn} \cdot \hat{s}_2 \rangle + \ldots + \langle (\hat{s}_1 \cdot \hat{s}_{b1})$$
$$\times (\hat{s}_{b1} \cdot \hat{s}_{b2}) \ldots (\hat{s}_{bn} \cdot \hat{s}_2) \rangle \tag{5}$$

$$= 1 + \langle (\hat{s}_1 \cdot \hat{s}_{b1})(\hat{s}_{b1} \cdot \hat{s}_{b2}) \ldots (\hat{s}_{bn} \cdot \hat{s}_2) \rangle = 1 + \frac{1}{3^n}m_S^2, \tag{6}$$

since all terms with at least one odd order power in $(\hat{s}_{bi} \cdot \hat{z})$ vanish. Accordingly, the low field magnetoconductance is strongly reduced in a higher order tunneling process, since a significant fraction of the spin polarization is lost in the transit via the localized states.

In order to compare this result with the experimental data, the following approach is used. Let $f_n(T)$ denote the fraction of charge carriers entering the nth order inelastic channel. Then by definition
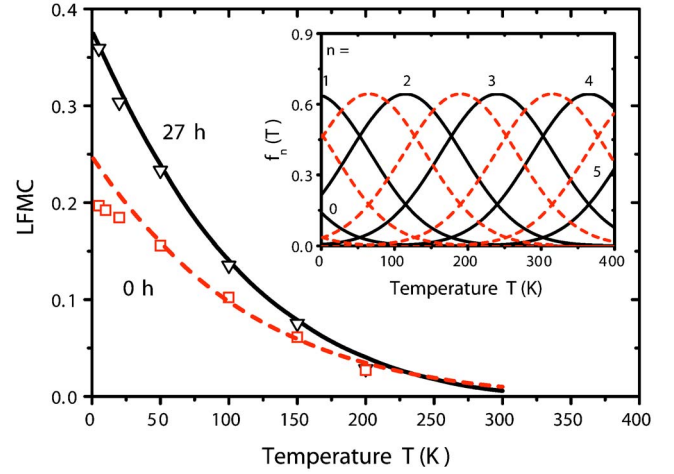

FIG. 3. (Color online) Simulated low field magnetoconductance using the model outlined in the text. For comparison the data of the 0 and 27 h milled samples are included. The inset shows the temperature profiles assumed for the nth order processes with solid (dashed) lines indicating the processes of the 27 h (0 h) milled LSMO powder. The Gaussians are centered at $T_n = -185\ \text{K} + n \times 125\ \text{K}$ (0 h) and $T_n = -135\ \text{K} + n \times 125\ \text{K}$ (27 h), respectively, with a width of 77.5 K.

$$\sum_{n=0}^{\infty} f_n(T) = 1 \tag{7}$$

and

$$\text{LFMC} = m_S^2 \sum_{n=0}^{\infty} f_n(T)/3^n. \tag{8}$$

At higher temperature more inelastic channels are available. Figure 3 shows a model calculation for the temperature dependence of the LFMC assuming a set of Gaussian functions centered in different temperature intervals (as seen in the inset) and corresponding to nth order tunneling processes. m_S^2 was taken from measurements. The low field magnetoconductance of the 0 and 27 h samples is shown in Fig. 3 for comparison. The strong decrease of the calculated LFMC is in good agreement with the experimental data.

The choice of Gaussian profiles centered in specific temperature intervals is somewhat arbitrary and idealized. The LFMC data only show that the fraction of higher order tunneling processes must increase with increasing temperature. It might prove possible in further studies to extract the distributions $f_n(T)$ by a simultaneous analysis of the LFMC and the nonlinear current-voltage characteristics. The latter have been analyzed in some systems containing only a few grain boundaries[3,15] using a model of inelastic tunneling through a barrier containing defects with a constant density of states.[16] The validity of this model for double exchange systems will have to be checked. In the pressed powder samples investigated here the number of junctions between the voltage contacts is so large that the voltage drop per junction is very small and only the linear response regime can be probed.

B. High field regime

The conductivity in the high field case is more difficult to calculate, since the magnetic field induces some magnetic order in the grain-boundary region, which—in turn—leads to stronger correlations. The average spins in the grains are again written as $\hat{s}_i = m_S \hat{z}$, whereas for the grain-boundary spins we assume a magnetically ordered part along the field direction as well as a random part (compare[17])

$$\hat{s}_b = m_{gb}\hat{z} + (1 - m_{gb}^2)^{1/2}\hat{r} \tag{9}$$

with

$$\hat{r}^2 = 1, \tag{10}$$

$$\langle \hat{r} \rangle = 0. \tag{11}$$

$m_{gb} \equiv M_{gb}(H,T)/M_{gbS}(0)$ is the grain-boundary magnetization $M_{gb}(H,T)$ normalized to its saturation value at $T=0$ K. In this approach only the average value of a grain-boundary spin is equal to unity

$$\langle \hat{s}_b^2 \rangle = m_{gb}^2 + (1 - m_{gb}^2) + 2m_{gb}(1 - m_{gb}^2)^{1/2}\langle \hat{z} \cdot \hat{r} \rangle = 1. \tag{12}$$

A lengthy calculation yields for the conductance σ_n of the nth order tunneling process in the high field limit

$$\sigma_0 \propto 1 + m_S^2, \tag{13}$$

$$\sigma_1 \propto 1 + 2m_S m_{gb} + \tfrac{1}{3}m_S^2 + \tfrac{2}{3}m_S^2 m_{gb}^2, \tag{14}$$

$$\sigma_2 \propto 1 + \tfrac{8}{3}m_S m_{gb} + \tfrac{1}{9}m_S^2 + m_{gb}^2 + \tfrac{13}{9}m_S^2 m_{gb}^2 + \tfrac{4}{3}m_S m_{gb}^3 + \tfrac{4}{9}m_S^2 m_{gb}^4, \tag{15}$$

$$\sigma_3 \propto 1 + \tfrac{26}{9}m_S m_{gb} + \tfrac{1}{27}m_S^2 + O(m_{gb}^2). \tag{16}$$

These equations show that for an elastic tunneling process ($n=0$) there is no high field magnetoconductance (MC) slope, whereas inelastic tunneling processes induce a high field MC slope. For an antiferromagnetically ordered or magnetically frustrated grain-boundary region it is reasonable to assume a linear field dependence of the grain-boundary magnetization

$$m_{gb} = \chi_{gb}B, \tag{17}$$

where χ_{gb} is the grain-boundary susceptibility normalized to the grain-boundary saturation magnetization. Inelastic tunneling processes lead to a conductance term linear in m_{gb} which explains the linear magnetic field dependence of the magnetoconductance observed experimentally. The coefficient C_n of this first order term depends on the order of the tunneling process with $C_0=0$, $C_1=2$, $C_2=8/3$, $C_3=26/9$, which can be generalized to $C_n=(3^n-1)/3^{n-1}$. Furthermore, higher order terms in m_{gb} appear already in the first order tunneling process which should lead to deviations from the linear field dependence of the magnetoconductance. In the limit $m_{gb}=0$ the low field magnetoconductance is correctly reproduced.

With the temperature profiles for the nth order tunneling processes introduced above, the slope of the high field con-
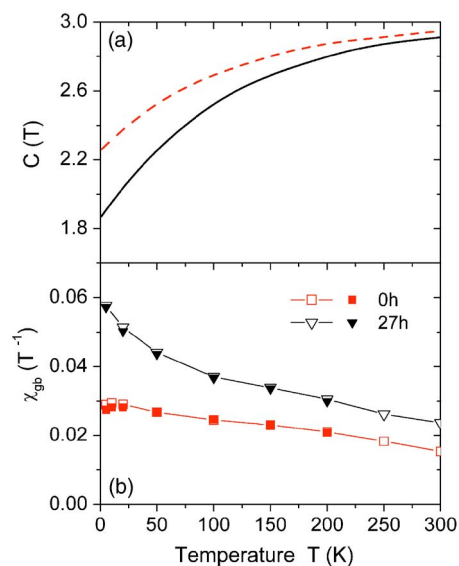

FIG. 4. (Color online (a) Coefficient $C(T)$ of the magnetoconductance term linear in the grain-boundary magnetization. $C(T)$ was calculated using the temperature profiles of the nth order tunneling contribution as shown in Fig. 3. Solid (dashed) line is for milling times of 27 h (0 h). (b) Grain-boundary susceptibility χ_{gb}. The data represented by the open symbols are derived from the magnetoconductance slope and $C(T)$, see Eq. (18), the data represented by the solid symbols were obtained from the magnetoconductance slope and LFMC, see Eq. (19).

ductivity $d\sigma/dB$ normalized to the zero field conductivity $\sigma(0)$ can be expressed as

$$\frac{1}{\sigma(0)}\frac{d\sigma}{dB} = m_S\chi_{gb}\sum_{n=0}^{\infty} C_n f_n(T) = 3m_S\chi_{gb}\sum_{n=0}^{\infty}\frac{3^n-1}{3^n}f_n(T) \tag{18}$$

$$= 3m_S\chi_{gb}\left[1 - \sum_{n=0}^{\infty}\frac{f_n(T)}{3^n}\right] = 3m_S\chi_{gb}\left[1 - \frac{\text{LFMC}}{m_S^2}\right]. \tag{19}$$

This offers us two methods to derive the grain-boundary susceptibility. In the first we use the temperature profiles from the LFMC analysis above and calculate the effective high field coefficient

$$C(T) = \sum_{n=0}^{\infty} C_n f_n(T), \tag{20}$$

which is shown in Fig. 4(a). Using this coefficient, the grain-boundary susceptibility χ_{gb} was calculated from the measured high field slope using Eq. (18) and neglecting higher order terms in m_{gb}. The results are presented as open symbols in Fig. 4(b) for the samples milled 0 and 27 h. χ_{gb} shows a linear temperature dependence with a paramagnetic upturn at low temperatures.

In the second method we use Eq. (19) and determine the grain-boundary susceptibility from the measured low field magnetoconductance, saturation magnetization and high field conductivity slope

$$\frac{1}{\chi_{gb}} = \frac{3m_S\sigma(0)}{d\sigma/dB}\left[1 - \frac{\text{LFMC}}{m_S^2}\right]. \qquad (21)$$

The results of this analysis are shown as solid symbols in Fig. 4(b) for the 0 and 27 h milled samples. These are in excellent agreement with the results obtained by the first method. This proves the consistency of the model proposed.

IV. CONCLUSIONS

In this work a model for inelastic grain-boundary tunneling based on the double-exchange mechanism has been derived. The model is able to account for the strong decrease of the low field magnetoconductance as a function of temperature that is generally observed in manganites. Moreover, the grain boundary susceptibility could be determined as a function of temperature from the comparison of the calculated and measured high field magnetoconductance.

The model calculations were compared to measurements on pressed manganite samples produced from powders milled at various milling times from 0 to 27 h. The samples have a grain-boundary susceptibility and a low field magnetoconductance both increasing with milling time. Both observations might be attributed to changes in the grain-boundary structure and the temperature profile of the nth order tunneling processes. The model proposed here, however, does not allow to draw further conclusions on the microscopic details of these changes.

In the high field regime a linear field dependence of the magnetoconductance was observed in the manganite samples and reproduced by the model. However, the calculations show that higher order terms in the grain-boundary magnetization appear in the expressions for the magnetoconductance that should lead to observable deviations from the linear field dependence. In the model discussed here the maximum magnetoconductance of the nth order tunneling process (calculated for $n \leqslant 2$) is $MC_n = 2^n$. This might account for the high magnetconductance values observed in the high field experiments. Recent data show that in a range of polycrystalline manganite samples with nonoptimal Curie temperature significant magnetoconductance contributions quadratic in field appear[11] in agreement with our model, whereas experimental data on polycrystalline LSMO extending to high magnetic fields of 60 T show a linear field dependence and no signs of saturation.[9] These data indicate that the exchange interactions and magnetic structure of the grain-boundary depend on the type of doping, thus modifying the field dependence of the magnetoconductance in the high field regime. The correlation between exchange interactions, Curie temperature, and grain-boundary magnetoconductance will be further studied in future work.

[1] M. Ziese, Rep. Prog. Phys. **65**, 143 (2002).

[2] J. E. Evetts, M. G. Blamire, N. D. Mathur, S. P. Isaac, B.-S. Teo, L. F. Cohen, and J. L. MacManus-Driscoll, Philos. Trans. R. Soc. London, Ser. A **356**, 1593 (1998).

[3] R. Gross, L. Alff, B. Buechner, B. H. Freitag, C. Hoefener, J. Klein, Y. Lu, W. Mader, J. B. Philipp, M. S. R. Rao, P. Reutler, S. Ritter, S. Thienhaus, S. Uhlenbruck, and B. Wiedenhorst, J. Magn. Magn. Mater. **211**, 150 (2000).

[4] M.-H. Jo, N. D. Mathur, N. K. Todd, and M. G. Blamire, Phys. Rev. B **61**, R14905 (2000).

[5] M. Bibes, L. Balcells, J. Fontcuberta, M. Wojcik, S. Nadolski, and E. Jedryka, Appl. Phys. Lett. **82**, 928 (2003).

[6] J. Inoue and S. Maekawa, Phys. Rev. B **53**, R11927 (1996).

[7] S. Lee, H. Y. Hwang, B. I. Shraiman, W. D. Ratcliff II, and S.-W. Cheong, Phys. Rev. Lett. **82**, 4508 (1999).

[8] M. Ziese, Phys. Rev. B **60**, R738 (1999).

[9] N. Kozlova, K. Dörr, D. Eckert, T. Walter and K.-H. Müller, J.

Magn. Magn. Mater. **261**, 48 (2003).

[10] J.-H. Park, E. Vescovo, H.-J. Kim, C. Kwon, R. Ramesh, and T. Venkatesan, Phys. Rev. Lett. **81**, 1953 (1998).

[11] R. B. Gangineni, K. Dörr, K. Nenkov, K.-H. Müller, and L. Schultz (unpublished).

[12] I. Panagiotopoulos, N. Moutis, M. Ziese, and A. Bollero (unpublished).

[13] J. M. D. Coey, A. E. Berkowitz, L. Balcells, F. F. Putris, and A. Barry, Phys. Rev. Lett. **80**, 3815 (1998).

[14] J. Klein, C. Höfener, S. Uhlenbruck, L. Alff, B. Büchner, and R. Gross, Europhys. Lett. **47**, 371 (1999).

[15] M. Paranjape, J. Mitra, A. K. Raychaudhuri, N. K. Todd, N. D. Mathur, and M. G. Blamire, Phys. Rev. B **68**, 144409 (2003).

[16] L. I. Glazman and K. A. Matveev, Zh. Eksp. Teor. Fiz. **94**, 332 (1988) [Sov. Phys. JETP **67**, 1276 (1988)].

[17] R. Skomski, in *Spin Electronics*, edited by M. Ziese and M. J. Thornton (Springer, Heidelberg, 2001), Chap. 10, p. 204.